ECS Transactions, 3 (1) 1095-1104 (2006)
10.1149/1.2356229, copyright The Electrochemical Society

Numerical Investigation of Water Transport in the PEMFC Components

V. Gurau, T. A. Zawodzinski, Jr. , J. A. Mann, Jr.

Chemical Engineering Department, Case Western Reserve University, Cleveland, Ohio 44106, USA

There are two competing mechanisms of water transfer between the ionomer distributed in the catalyst layer and the catalyst layer pores; these are: (*i*) sorption/desorption and (*ii*) water dragged by the protons engaged in the electrochemical reaction (the secondary current). The level at which water accumulates in GDLs is determined by the saturation equilibrium at the GDL-channel interface. The level at which water accumulates in the catalyst layer is determined by the GDL permeability and the saturation equilibrium at the GDL-catalyst layer interface. In the cathode flow domain mass is overall produced by (*i*) mass of protons crossing the double-layer and (*ii*) mass of water transferred between the ionomer distributed in the catalyst layer and the catalyst layer pores; for this reason the homogeneous multi-phase models based on the two-phase mixture model are inadequate to describe two-phase phenomena in PEMFCs. We propose a multi-phase, multi-fluid model that captures these phenomena.

1. Introduction

There are many reasons why the solution for the transport equations describing two-phase phenomena in fuel cell catalyst layers has been traditionally difficult to obtain. Firstly, the most frequently used *homogeneous multi-phase models* (1-8) which are based on Wang's *two-phase mixture model* developed earlier for other applications (9-11) are valid only when no mass is overall produced or consumed in the domain. In the *flow domain* of a PEM fuel cell cathode, for each eight units of mass of oxygen consumed per second in the electrochemical reaction, nine units of mass of water are produced (the difference is the mass of protons entering the flow domain from the *solid* ionomer). In addition, water is 'produced' in the cathode catalyst layer as result of water transfer between ionomer and the catalyst layer pores. Secondly, it has not been clear how the source terms for water production as a result of water transfer between ionomer and catalyst layer pores were to be expressed in the catalyst layer. Thirdly, it has not been easy to resolve numerically the saturation discontinuity at the catalyst layer - gas diffusion layer (GDL) interface when the two porous media are characterized by different drainage / imbibition curves.

The answer to these concerns is to use *a multi-fluid, multi-phase model* as the one presented here and to solve individual transport equations for each phase. There have been published a handful of papers describing multi-phase transport in PEM fuel cells using the multi-fluid approach (12-15) but no one included the catalyst layer(s) in the model. Interestingly, the only published papers we could find that attempt to incorporate the catalyst layer(s) are the ones that use the two-phase mixture model (2, 6-8), *i.e.* the ones that for the reason mentioned above cannot simulate two-phase transport in PEM fuel cell catalyst layers. For this reason probably, both Wang's and Liu's works consider

rather surprisingly, that no mass is overall produced or consumed in catalyst layers by electrochemical reaction and water transfer between catalyst layer pores and ionomer (in their models the source term in the continuity equation for catalyst layers is zero). Accordingly, no one of the cited papers present liquid water saturation or water content profiles in the catalyst layer(s). These models consider tacitly single-phase transport in the catalyst layer and enforce the saturation in the catalyst layer. In addition, they do not consider saturation equilibrium at channel-GDL and GDL-catalyst layer interfaces. With these limitations the models cannot predict even qualitatively the two-phase transport and equilibrium in PEM fuel cells.

2. Model Description

The 3-D multi-phase (multi-fluid), multi-component, transient model described here accounts for each phase momentum and species (O_2, H_2O, N_2) transport in the cathode channel, GDL and catalyst layer and for the current density, ionomer-phase potential and water content in the catalyst layer and membrane. The model is capable of predicting liquid water accumulation at the channel - GDL interface and the saturation discontinuity at the GDL – catalyst layer interface. The model accounts for the liquid water produced as a result of (*i*) electrochemical reaction, (*ii*) two-phase change and (*iii*) water transfer between the ionomer distributed in the catalyst layer and the catalyst layer pores. To account for the water transport in the ionomer-phase of the CCM we have developed a transport equation for the water content - λ. The source / sink terms of the newly developed transport equation represent the parallel mechanisms of water transfer between ionomer and the catalyst layer pores; at cathode they are: (*i*) sorption / desorption and (*ii*) proton drag generated by the secondary current, while at the interface with the anode it is only sorption / desorption .

The proposed model considers separate transport equations associated with each phase. The continuity, momentum and species equations are written below for the entire flow domain. The terms that are particular to a certain sub-domain are multiplied by the step function δ_Ω defined as:

$$\delta_\Omega = \begin{cases} 1 & \text{in } \Omega \\ 0 & \text{outside } \Omega \end{cases} \quad [1]$$

where the domain Ω can be either the catalyst layer, the GDL, the channel or any reunion of them. We also use the step function $\delta(x)$ defined as:

$$\delta(x) = \begin{cases} 1 & \text{if } x \geq 0 \\ 0 & \text{if } x < 0 \end{cases} \quad [2]$$

The porosity is therefore defined for the entire flow domain using the δ_Ω step function:

$$\varepsilon = \delta_{CL} \cdot \varepsilon_{CL} + \delta_{GDL} \cdot \varepsilon_{GDL} + \delta_{CH} \cdot 1 \quad [3]$$

where the subscripts *CL*, *GDL* and *CH* stand for the catalyst layer, the GDL and the channel, respectively.

2.1. Continuity Equations

The continuity equations for the gas and liquid phases are:

$$\frac{\partial\left[\varepsilon s_g \rho_g\right]}{\partial t} + \nabla \cdot \left[\varepsilon s_g \rho_g \vec{U}_g\right] = \dot{m}_g \qquad [4a]$$

$$\frac{\partial\left(\varepsilon s_l \rho_l\right)}{\partial t} + \nabla \cdot \left(\varepsilon s_l \rho_l \vec{U}_l\right) = \dot{m}_l \qquad [4b]$$

where the rates of mass production are

$$\begin{aligned}\dot{m}_g = & \underbrace{\varepsilon \cdot \left(s_l \dot{m}_{evap} - s_g \dot{m}_{cond}\right)}_{I} + \\ & + \underbrace{\delta_{CL} \cdot \varepsilon \cdot \left[\delta\left(Y^{sat}_{H_2O} - Y_{H_2O}\right) \cdot s_g \dot{m}_{electrochem}\right]}_{II} + \\ & + \underbrace{\delta_{CL} \cdot \varepsilon \cdot \left[-s_g \dot{m}_{sorption} + \delta\left(Y^{sat}_{H_2O} - Y_{H_2O}\right) \cdot \left(\dot{m}_{desorption} + \dot{m}_{\text{sec}ondary\ current}\right)\right]}_{III}\end{aligned} \qquad [4c]$$

$$\begin{aligned}\dot{m}_l = & \underbrace{\varepsilon \cdot \left(-s_l \dot{m}_{evap} + s_g \dot{m}_{cond}\right)}_{I} + \\ & + \underbrace{\delta_{CL} \cdot \varepsilon \cdot \left[\delta\left(Y_{H_2O} - Y^{sat}_{H_2O}\right) \cdot s_g \dot{m}_{electrochem}\right]}_{II} + \\ & + \underbrace{\delta_{CL} \cdot \varepsilon \cdot \left[-s_l \dot{m}_{sorption} + \delta\left(Y_{H_2O} - Y^{sat}_{H_2O}\right) \cdot \left(\dot{m}_{desorption} + \dot{m}_{\text{sec}ondary\ current}\right)\right]}_{III}\end{aligned} \qquad [4d]$$

The continuity equations show that each phase may be created or consumed by: (*I*) change of phase, (*II*) electrochemical reaction and (*III*) transfer between catalyst layer pores and ionomer.

We will demonstrate in section 2.3 that there are two parallel mechanisms for water transfer between the ionomer, which is distributed in the catalyst layer and the catalyst layer pores; these are: (*i*) by sorption / desorption and (*ii*) by water dragged by the protons engaged in the electrochemical reaction (the secondary current). The first one is a two-way process while the second one transfers water only from the ionomer to the catalyst layer pores. When no current passes through the CCM, the water content, λ in ionomer is in equilibrium with the water vapor at its local activity and/or the liquid water present in the catalyst layer pores according to isopiestic curves (16). When this equilibrium is perturbed water will be transferred between ionomer and catalyst layer pores by sorption or desorption until a new equilibrium is reached. This process is most probably diffusion controlled since the time necessary for water to diffuse from the ionomer-pore interface to the ionomer core is relatively long (a few hundred seconds according to Figure 3 in reference (16)). The rate of sorption / desorption which must be

determined experimentally is an odd function of the offset from equilibrium $\left(\lambda - \lambda_{equilibrium}\right)$:

$$\dot{m}_{sorption} = -\dot{m}_{desorption} = -f\left(\lambda - \lambda_{equilibrium}\right)\frac{\rho_{dry}}{EW}MW_{H_2O} \qquad [5]$$

where λ is the actual water content in ionomer and $\lambda_{equilibrium}$ is the value at equilibrium defined by the isopiestic curve.

The rate at which water is dragged out from ionomer into the catalyst layer pores by the protons engaged in the electrochemical reaction (the secondary current) is:

$$\dot{m}_{\text{sec}ondary\ current} = n_{drag}\frac{\left(a \cdot i_0\right)_{cathode}}{F}\frac{\rho_{dry}}{EW}MW_{H_2O} \qquad [6]$$

and will be derived in section 2.3.

By adding the continuity equations [4a] and [4b] one obtains the continuity equation for the mixture fluid as defined in Wang's two-phase mixture model (9-11). It is important to notice that by adding these equations only the source terms standing for the change of phase cancel out. The continuity equation for the mixture fluid has a non-zero source term standing for: (*i*) the rate at which the mass of protons enters the flow domain from the solid ionomer during the electrochemical reaction and (*ii*) the rate at which the mass of water is transferred between pores and ionomer. Wang's two-phase mixture model was derived assuming that no mass is overall produced or consumed in the domain. We believe therefore that the two-phase mixture model, in the form presented (9-11) is not appropriate to simulate two-phase transport in PEM fuel cell electrodes.

2.2. Momentum Equations

The momentum equations for the gas and liquid phases are:

$$\frac{\partial\left[\varepsilon s_g \rho_g \vec{U}_g\right]}{\partial t} + \nabla\cdot\left[\varepsilon s_g \rho_g \vec{U}_g \otimes \vec{U}_g\right] - \nabla\cdot\left[\varepsilon s_g \mu_g \nabla\vec{U}_g\right] = \varepsilon s_g\left(-\nabla p_g + \vec{B}_g\right) + \dot{m}_g \vec{U}_g \qquad [7a]$$

$$\frac{\partial\left[\varepsilon s_l \rho_l \vec{U}_l\right]}{\partial t} + \nabla\cdot\left[\varepsilon s_l \rho_l \vec{U}_l \otimes \vec{U}_l\right] - \nabla\cdot\left[\varepsilon s_l \mu_l \nabla\vec{U}_l\right] = \varepsilon s_l\left(-\nabla p_l + \vec{B}_l\right) + \dot{m}_l \cdot \vec{U}_l \qquad [7b]$$

The liquid pressure p_l in porous media is the gas pressure p_g plus the capillary pressure. The capillary pressure, p_c depends locally on the nature of the solid matrix (in terms of the contact angle and surface energy) and on the degree of saturation, s_l. While it is necessary to determine experimentally the capillary pressure – saturation relationship for each GDL and catalyst layer, in the present calculations we assumed an arbitrary function $p_c = p_c\left(s_l\right)$. The capillary pressure gradient is then calculated as:

$$\nabla p_c = \frac{dp_c}{ds_l} \nabla s_l \qquad [8]$$

2.2.1. Numerical Treatment of the GDL-Catalyst Layer Interface. At the catalyst layer – GDL interface p_g , p_l and therefore p_c must be continuous which means that a discontinuity must exist for s_l . In the numerical code, for the catalyst layer and GDL sub-domains the capillary pressure gradient is calculated using [8]. At interface the capillary pressure gradient is discretized as:

$$\nabla p_c = \frac{p_c^i - p_c^{i-1}}{y^i - y^{i-1}} \qquad [9]$$

where p_c is calculated using $p_c = p_c(s_l)$ (different on each side of the interface), y is the direction normal to the interface, and i and $i-1$ are adjacent grid points, one on each side of the interface. As a requirement for continuity the numerical code always insures that p_g is continuous. The gradient term [9] has the effect of displacing liquid from one side of the interface to the other until p_c is the same on both sides.

2.2.2. Numerical Treatment of the GDL-Channel Interface. When liquid water exits the GDL it forms pending or sessile droplets which remain attached to the GDL surface as long as the gravity and the shear forces generated by two-phase drag do not exceed the force available to support them. In this model we adopted the Tate's law as condition for droplet detachment (see for example (17)):

At GDL – channel interface the water pressure downstream of the capillaries is equal to the pressure in the attached droplets which they feed. The pressure in the droplet is expressed by the Young-Laplace equation. As water initially flows out from the capillaries, the radius of the bulge decreases to a minimum equal to the capillary radius, than increases again (see Figure 1). The maximum pressure corresponding to the minimum radius of the bulge is the pressure which the water inside the GDL must exceed at interface before it can further leave the GDL. Liquid water will therefore accumulate in the GDL without leaving it until this maximum pressure is achieved. In the numerical code the liquid pressure in the control volumes adjacent to the GDL is set as a function of the droplet radius as given by the Young-Laplace equation. Assuming the droplets are spherical, the radius of the attached droplets is calculated as a function of the liquid mass.

At GDL – channel interface the pressure gradient term in equation [7b] is discretized as:

$$\nabla p_l = \frac{p_l^i - p_l^{i-1}}{y^i - y^{i-1}} \qquad [10]$$

where the value of p_l in channel is given by Young-Laplace equation, *i* and *i-1* denote adjacent control volumes, one on each side of the interface and y is the distance normal to the interface.

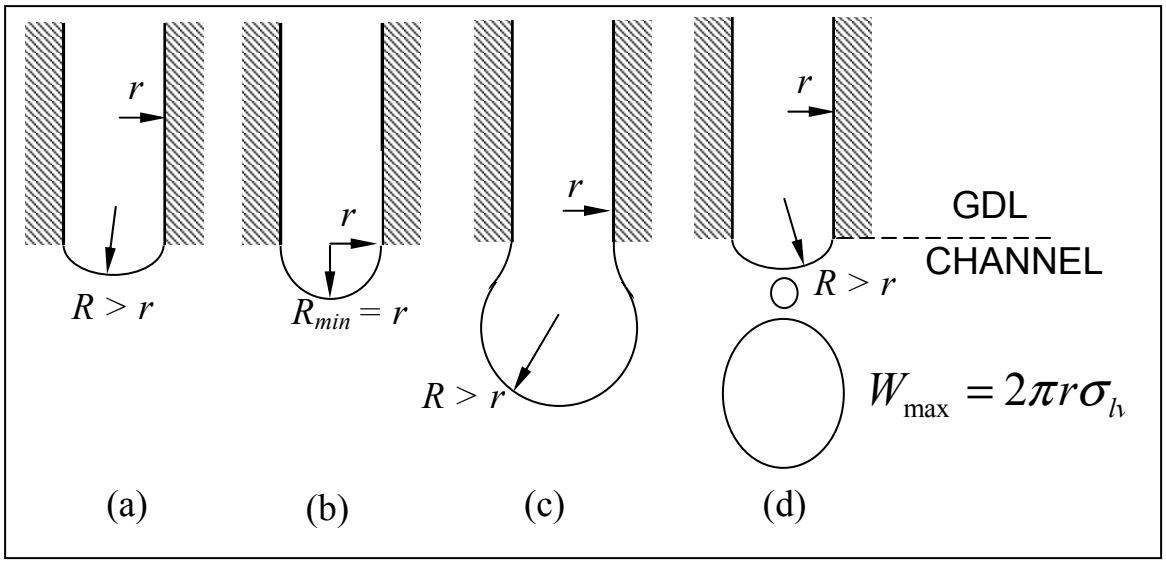

Figure 1. The radius of the attached bulge, R decreases to a minimum equal to the capillary radius, r. Liquid water accumulates in the GDL until $p_l = p_l^{\max} = \frac{2\sigma_{lv}}{r}$ *at interface. The pendant drop detaches when its weight exceeds* $2\pi r\sigma_{lv}$

In the numerical code gravity and two-phase drag are set as body forces everywhere in the channel except in the control volumes adjacent to the GDL where the droplets are attached. When in such a control volume the weight of the accumulated liquid exceeds the value prescribed by Tate's law the corresponding mass and its momentum are moved below into the adjacent control volume where gravity and two-phase drag act. This is done by setting additional negative source terms for the mass and momentum equations [4b] and [7b] in the control volumes adjacent to the GDL and identical but positive source terms in the next layer of control volumes adjacent to the former. After the liquid is transferred to the adjacent layer of control volumes it will be transported by gravity and two-phase drag.

2.3. Equation for Conservation of Charge and Transport Equation for Water Content in Ionomer

The equation for the conservation of charge derives from the transport equation for proton migration and has the form:

$$\begin{cases} \nabla \cdot \vec{i} = \left(a \cdot i_0\right)_{cathode} & \text{at cathode} \\ \nabla \cdot \vec{i} = 0 & \text{in membrane} \\ \nabla \cdot \vec{i} = \left(a \cdot i_0\right)_{anode} & \text{at anode} \end{cases} \qquad [11]$$

It states that current density is produced in the anode catalyst layer at a volumetric rate of $\left(a \cdot i_0\right)_{anode}$, no current density is consumed or produced in membrane, and current density is consumed in the cathode catalyst layer at a volumetric rate of $\left(a \cdot i_0\right)_{cathode}$. The current density consumed in the cathode catalyst layer is related to the protons that engage in the

electrochemical reaction, *i.e.* the protons that cross the double-layer from the ionomer to the platinum sites. The protons crossing the double-layer generate the secondary current density, while the primary current density is generated by the protons migrating inside the ionomer. As the protons migrating in the cathode catalyst layer along the ionomer exit the ionomer towards the reaction sites, the primary current density decreases from the constant value in the membrane to zero at the interface with the GDL.

In the ionomer-phase of a CCM water is transported by proton drag and back-diffusion. The water flux through the membrane is (18):

$$\vec{N}_{H_2O} = n_{drag} \cdot \frac{\vec{i}}{F} + \frac{\rho_{dry}}{EW} D_\lambda \nabla \lambda \qquad [12]$$

The drag coefficient n_{drag} was measured (19, 20) for membranes immersed in liquid water ($n_{drag} = 2.5$) and for membranes at equilibrium with water vapor over a wide range of activities ($n_{drag} = 1$). The intra-diffusion coefficient of water D_λ is a function of water content (18). The water content, λ is a transportable parameter. Its transport equation can be obtained by performing its flux balance over a control volume:

$$\frac{\partial \lambda}{\partial t} + \frac{\rho_{dry}}{EW} \nabla \left(D_\lambda \nabla \lambda \right) = \left(\dot{\lambda} - n_{drag} \frac{\nabla \vec{i}}{F} \right) \qquad [13]$$

where the term containing ∇n_{drag} cancels since $n_{drag} = 1$.

$\dot{\lambda}$ represents the volumetric rate of water content transferred between the ionomer distributed in the catalyst layer and the catalyst layer pores by sorption / desorption when the equilibrium is perturbed and when no current passes through the membrane. It must be determined experimentally and can be represented by an odd function of the offset from equilibrium, $\left(\lambda - \lambda_{equilibrium} \right)$, where λ is the actual water content in the ionomer and $\lambda_{equilibrium}$ is the value at equilibrium defined by the isopiestic curves (see also equation [5]):

$$\dot{\lambda}_{sorption} = -\dot{\lambda}_{desorption} = f\left(\lambda - \lambda_{equilibrium} \right) \qquad [14]$$

The second source term in the transport equation [13], $-n_{drag} \frac{\nabla \vec{i}}{F}$ is zero in the membrane and non-zero in the catalyst layers (see equation [11]). Since at cathode the term $\frac{\nabla \vec{i}}{F}$ represents the volumetric rate at which protons exit the ionomer towards the reaction sites it is easy to interpret the second source term as the volumetric rate at which water content is dragged out by protons as they engage in the electrochemical reaction (the secondary current). From equation [11] at cathode this source term is (see also equation [6]):

$$\dot{\lambda}_{secondary\ current} = -n_{drag} \frac{\left(a \cdot i_0 \right)_{cathode}}{F} \qquad [15]$$

At anode protons bond with one water molecule forming hydronium ions (H_3O^+) then migrate towards the cathode. At the cathode reaction sites the hydronium ions cross the double layer and release the water molecule as the proton engages in the electrochemical reaction on the platinum surface. In this context, the second source term can be interpreted as the volumetric rate at which the hydronium ions cross the interface.

At cathode water can be transferred between ionomer and catalyst layer pores in both directions by the sorption / desorption mechanism. The second mechanism always transfers water from the ionomer to the catalyst layer pores. It is therefore possible, in particular at high current densities that the water content at cathode to be lower than predicted by the LANL group when no current passes through the CCM. Indeed, as was discussed above, the sorption / desorption process is slower since it is most probably diffusion controlled.

At anode the second source term in the transport equation [13] should be zero since protons crossing the interface in the opposite direction, (from the platinum sites to the ionomer) do not drag water and the hydronium ions form only after the protons enter in the ionomer-phase. At anode therefore, water is transferred between the ionomer and catalyst layer pores only by sorption / desorption.

3. Results and Discussion

The system of transport equations [4a], [4b], [7a], [7b], [13] and the transport equations for the ionomer-phase potential and for the species conservation (not shown) was solved using the ANSYS CFX4.4 software. We have developed a library of user-FORTRAN subroutines to adapt the particular equations to the general form solved by the software. The software uses the Inter-Phase Slip Algorithm (IPSA) of Spalding.

We performed a transient analysis of the two-phase phenomena using a time step of 100 ms and considering two cases, one for relatively low and the other for relatively high (three times higher than the former) GDL permeability coefficients. Simulations were carried out for a total of 60 seconds of fuel cell operation: 10 seconds each at 0.75V, 0.72V, 0.69V, 0.67V and 20 seconds at 0.65V.

The initial liquid saturation level was constant throughout of the GDL and the same for both cases, $s_l = 0.3$. The corresponding initial saturation level in the catalyst layer was set using the constraint $p_c^{GDL} = p_c^{CL}$ and the expressions $p_c = p_c(s_l)$ on both sides of the interface. The initial water content level was constant throughout the CCM and the same for both cases, $\lambda = 14.93$ which corresponds to the initial saturation and a water vapor activity of 1 in the catalyst layer.

As gas phase is initially consumed in the electrochemical reaction (water product is in liquid form since supersaturated condition is present) a negative gas pressure gradient establishes from channel to the catalyst layer which drives liquid water towards the catalyst layer and above the flow-field rib. Liquid water accumulates there until enough capillary pressure gradient builds up to oppose the adverse effect of the gas pressure gradient. At this time the water produced in catalyst layer starts to flow out of the catalyst layer into the GDL.

In Figure 2 are shown the liquid saturation profiles in GDL and catalyst layer along a line passing through the symmetry plane of the channel and 1 cm downstream of the inlet, at different time intervals. Liquid saturation increases in the catalyst layer as water is produced and approaches a steady-state level. As it flows out of the catalyst layer,

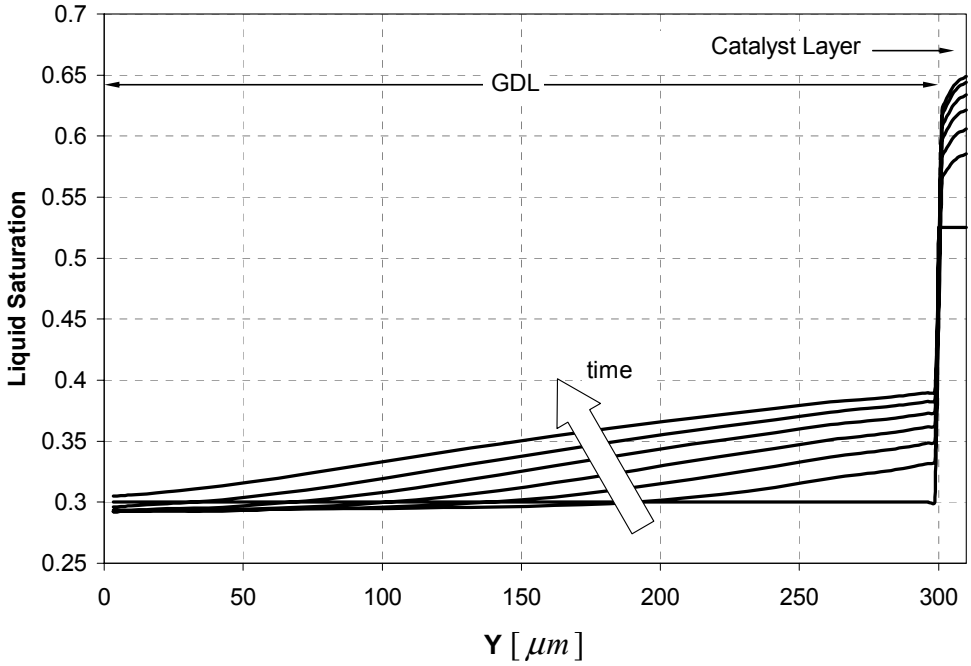

Figure 2. Liquid saturation profiles after 0, 10, 20, 30, 40, 50, and 60 seconds of fuel cell operation, along a line in the symmetry plane of the channel, 1 cm downstream of the inlet. The case is for a GDL with the following permeability coefficients: $(k_{V,in-plane} = 2.0E-12m^2, k_{V,through-plane} = 2.5E-12m^2)$

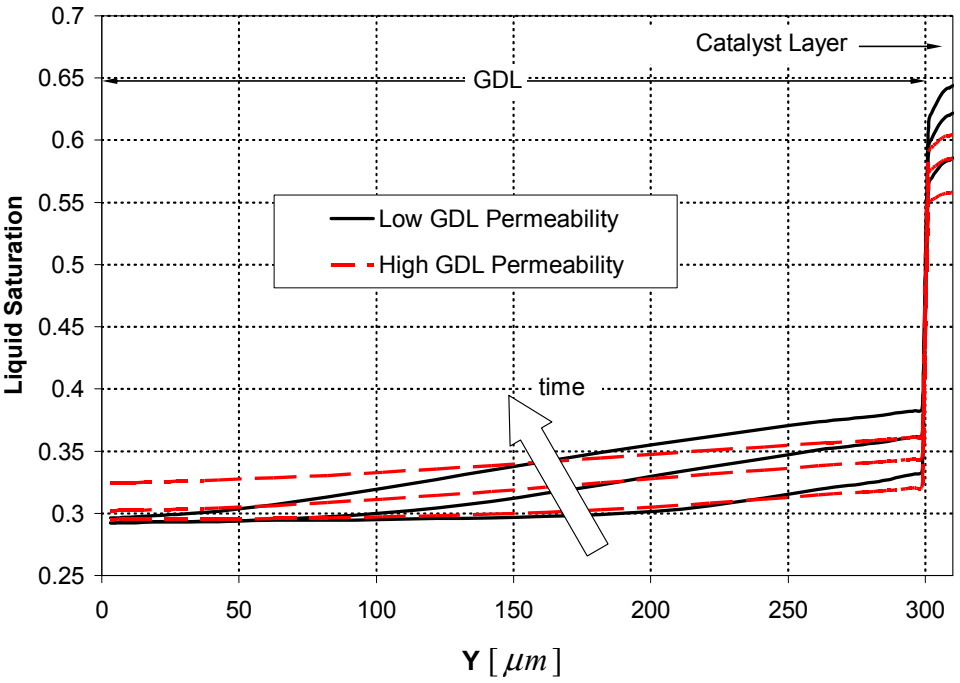

Figure 3. Liquid water saturation profiles after 10, 30 and 50 seconds of fuel cell operation for the case of a GDL with relatively low permeability coefficients $(k_{V,in-plane} = 2.0E-12m^2, k_{V,through-plane} = 2.5E-12m^2)$ *and a GDL with relatively high permeability coefficients* $(k_{V,in-plane} = 6.0E-12m^2, k_{V,through-plane} = 7.5E-12m^2)$

water accumulates in the GDL at a constant slope, which is determined by the permeability coefficients. It accumulates until the liquid pressure at the interface with the channel reaches the maximum pressure prescribed by the Young-Laplace equation when $R_{drop} = r_{pore}$ then starts to flow out of the GDL into the channel.

Figure 3 shows the liquid saturation profiles along the same line, for the case of two GDLs: one with relatively low permeability coefficients, and one with permeability coefficients three times higher than the former. Liquid water accumulates at higher saturation levels in the catalyst layer adjacent to the GDL with low permeability. This is the result of the saturation equilibrium that establishes at the interface. Since the slope of the liquid saturation profile is higher in the GDL with low permeability, the saturation level at the interface with the catalyst layer is higher than in the case of high GDL permeability. As a consequence, the liquid content in the catalyst layer will be higher. A low GDL permeability may prove beneficial in the case of a PEMFC operating at low relative humidity.

References

1. Z.H. Wang, C.Y. Wang and K.S. Chen, *J. Power Sourc.*, **94**, 40 (2001).
2. L. You and H.T. Liu, *Int. J. Heat Mass Transfer*, **45**, 2277 (2002).
3. S. Mazumder and J. V. Cole, *J. Electrochem. Soc.*, **150**, A1510 (2003).
4. U. Pasaogullari and C.Y. Wang, *J. Electrochem. Soc.*, **151**, A399 (2004).
5. U. Pasaogullari and C.Y. Wang, *Electrochimica Acta*, **49**, 4359 (2004).
6. U. Pasaogullari and C.Y. Wang, *J. Electrochem. Soc.*, **152**, A380 (2005).
7. H. Sun, H.T. Liu and L.J. Guo, *J. Power Sourc.*, **143**, 125 (2005).
8. L. You and H.T. Liu, *J. Power Sourc.*, **155**, 219 (2006).
9. C.Y. Wang and C. Beckermann, *Int. J. Heat Mass Transfer*, **36**, 2747 (1992).
10. C.Y. Wang and P. Cheng, *Int. J. Heat Mass Transfer*, **39**, 3607 (1996).
11. C.Y. Wang, *Numerical Heat Transfer B*, **31**, 85 (1997).
12. S. Shimpalee and S. Dutta, *Numerical Heat Transfer A*, **38**, 111 (2000).
13. D. Natarajan and T.V. Nguyen, *J. Electrochem. Soc.*, **148**, A1324 (2001).
14. T. Berning, D.M. Lu and N. Djilali, *J. Power Sourc.*, **106**, 284 (2002).
15. T. Berning and N. Djilali, *J. Electrochem. Soc.*, **150**, A1589 (2003).
16. T.A. Zawodzinski, C. Derouin, S. Radzinski, R.J. Sherman, V.T. Smith, T.E. Springer and S. Gottesfeld, *J. Electrochem. Soc.*, **140**, 1041 (1993).
17. A.W. Adamson and A.P. Gast, *Physical Chemistry of Surface*, p.20, John Wiley & Sons, New York (1997)
18. T.E. Springer, T.A. Zawodzinski, and S. Gottesfeld, in *Modeling of Batteries and Fuel Cells*, R.E. White, M.W. Verbrugge and J.F. Stockel, Editors, PV 91-10, p. 209, The Electrochemical Society Proceedings Series, Pennington, NJ (1990).
19. T.A. Zawodzinski, T.E. Springer, J. Davey, J. Valerio and S. Gottesfeld in *Modeling of Batteries and Fuel Cells*, R.E. White, M.W. Verbrugge and J.F. Stockel, Editors, PV 91-10, p. 187, The Electrochemical Society Proceedings Series, Pennington, NJ (1990).
20. T.A. Zawodzinski, J. Davey, J. Valerio and S. Gottesfeld, *Electrochimica Acta*, **40**, 297 (1995).